

AD-A198 153

CRYSTAL GROWTH AND MECHANICAL PROPERTIES OF  
SEMICONDUCTOR ALLOYS(U) STANFORD UNIV CA DEPT OF  
MATERIALS SCIENCE AND ENGINEERING D A STEVENSON

1/1

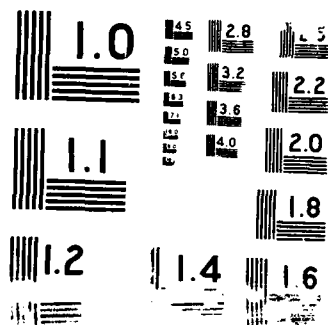
UNCLASSIFIED

14 APR 88 AFOSR-TR-88-0832 AFOSR-85-0158

F/G 7/2

NL





SECURITY CLASSIFICATION OF THIS PAGE

## REPORT DOCUMENTATION PAGE

1a. REPORT SECURITY CLASSIFICATION <b>UNCLASSIFIED</b>		1b. RESTRICTIVE MARKINGS													
2i. <b>AD-A198 153</b>		3. APPROXIMATE AVAILABILITY REPORT <b>distribution</b>													
4. <b>AD-A198 153</b>		5. MONITORING ORGANIZATION REPORT NUMBER(S) <b>AFOSR-TR- 88-0832</b>													
6a. NAME OF PERFORMING ORGANIZATION Dept of Material Sci & Eng Stanford University	6b. OFFICE SYMBOL (If applicable)	7a. NAME OF MONITORING ORGANIZATION AFOSR/NE													
6c. ADDRESS (City, State and ZIP Code) Stanford, CA 94305		7b. ADDRESS (City, State and ZIP Code) Bldg 410 Bolling AFB, DC 20332-6448													
8a. NAME OF FUNDING/SPONSORING ORGANIZATION AFOSR	8b. OFFICE SYMBOL (If applicable) NE	9. PROCUREMENT INSTRUMENT IDENTIFICATION NUMBER AFOSR-85-0158													
8c. ADDRESS (City, State and ZIP Code) Bldg 410 Bolling AFB, DC 20332-6448		10. SOURCE OF FUNDING NOS. <table border="1"><thead><tr><th>PROGRAM ELEMENT NO.</th><th>PROJECT NO.</th><th>TASK NO.</th><th>WORK UNIT NO.</th></tr></thead><tbody><tr><td>61102 F</td><td>2306</td><td>B1</td><td></td></tr></tbody></table>		PROGRAM ELEMENT NO.	PROJECT NO.	TASK NO.	WORK UNIT NO.	61102 F	2306	B1					
PROGRAM ELEMENT NO.	PROJECT NO.	TASK NO.	WORK UNIT NO.												
61102 F	2306	B1													
11. TITLE (Include Security Classification) CRYSTAL GROWTH & MECHANICAL PROPERTIES OF SEMICONDUCTOR ALLOYS															
12. PERSONAL AUTHOR(S) Dr Stevenson															
13a. TYPE OF REPORT Annual	13b. TIME COVERED FROM 15/04/87 TO 14/04/88	14. DATE OF REPORT (Yr., Mo., Day)	15. PAGE COUNT												
16. SUPPLEMENTARY NOTATION															
17. COSATI CODES <table border="1"><thead><tr><th>FIELD</th><th>GROUP</th><th>SUB. GR.</th></tr></thead><tbody><tr><td></td><td></td><td></td></tr><tr><td></td><td></td><td></td></tr><tr><td></td><td></td><td></td></tr></tbody></table>		FIELD	GROUP	SUB. GR.										18. SUBJECT TERMS (Continue on reverse if necessary and identify by block number)	
FIELD	GROUP	SUB. GR.													
19. ABSTRACT (Continue on reverse if necessary and identify by block number) The mechanical properties of semiconductor materials is a topic of practical and theoretical interest. The mechanical properties relate to the changes in electronic and optical properties that may accompany the processing of semiconductor materials into devices, particularly the introduction of dislocations upon thermal processing, slicing, polishing, ion implantation, and the application of films. <i>Thy...</i>															
20. DISTRIBUTION/AVAILABILITY OF ABSTRACT UNCLASSIFIED/UNLIMITED <input checked="" type="checkbox"/> SAME AS RPT. <input type="checkbox"/> DTIC USERS <input type="checkbox"/>		21. ABSTRACT SECURITY CLASSIFICATION <b>UNCLASSIFIED</b>													
22a. NAME OF RESPONSIBLE INDIVIDUAL <i>Halley</i>		22b. TELEPHONE NUMBER (Include Area Code) (202) 767-4932	22c. OFFICE SYMBOL NE												

DTIC  
ELECTE  
AUG 25 1988  
S E D

**AFOSR-TR. 88-0832**

Annual Report  
for  
April 15, 1987-April 14, 1988

for  
Contract AFOSR 85-0158  
Project Task 2306/B1

Crystal Growth and Mechanical Properties of  
Semiconductor Alloys

Principal Investigator: D. A. Stevenson  
Department of Materials Science and Engineering  
Stanford University  
Stanford, CA 94305

Sponsored by  
Air Force Office of Scientific Research

Accession For	
NTIS GRA&I	<input checked="" type="checkbox"/>
DTIC TAB	<input type="checkbox"/>
Unannounced	<input type="checkbox"/>
Justification	
By	
Distribution/	
Availability Codes	
Dist	Avail and/or Special



**A-1**

## I. Introduction

The mechanical properties of semiconductor materials is a topic of practical and theoretical interest. The mechanical properties relate to the changes in electronic and optical properties that may accompany the processing of semiconductor materials into devices, particularly the introduction of dislocations upon thermal processing, slicing, polishing, ion implantation, and the application of films. Furthermore, the mechanical strength is of chief concern in the physical handling of wafers during processing and in the integrity of devices during service. Recent theoretical studies have related hardness in ternary semiconductor alloys to fundamental atomic properties, but comparison with experiments is limited because of insufficient information [1].

In spite of this obvious interest, there has been relatively little work done on this topic. A major problem is the preparation of bulk samples for conventional mechanical tests. There is usually a large separation between the liquidus and solidus on the pseudobinary phase diagram of such systems, which causes segregation during melt growth [2]. Even worse is the tendency in these systems for interface breakdown, due to constitutional supercooling, thus making crystal growth difficult [2-6].

The objective of this research program is to explore methods for determining the mechanical properties of ternary semiconductor alloy systems. To achieve this objective, we are initially exploring three possible approaches: hardness measurements on thick films (10-100  $\mu\text{m}$ ) using conventional microhardness techniques; hardness measurements on thin films ( $< 1 \mu\text{m}$ ) using a nanoindenter; and hardness measurements and eventually bend tests on bulk samples. In the last twelve months, we have pursued these approaches with the following specific studies: an attempt to grow thick films of GaPAs by isothermal vapor phase epitaxy (ISOVPE); Vickers hardness measurements of ZnTe to add to the  $\text{Zn}_x\text{Cd}_{1-x}\text{Te}$  hardness versus composition curve; nanoindenter studies of  $\text{Hg}_{1-x}\text{Cd}_x\text{Te}$  and  $\text{Hg}_{1-x}\text{Zn}_x\text{Te}$  thin films and ZnTe-CdTe superlattices; and bulk growth, microprobe analysis, and microhardness measurements of  $\text{Ga}_x\text{In}_{1-x}\text{Sb}$ . Details of these activities are

provided below.

## II. Why measure hardness?

Before we describe the details of our research progress, we will first discuss the motivation for this study, "Why measure hardness in binary semiconductors and ternary semiconductor alloys?" As metallurgists point out [7-10], hardness measurements can be inexact and only measure the material's resistance to plastic flow or indentation. Mechanical tests such as tension or compression tests, bend tests, and fracture toughness tests are more revealing and should be used whenever possible. The problem with conventional tests is that large bulk samples are necessary. With the exception of Si and GaAs, there are very few semiconductors that are available in large single crystals; most are available only as thin films on substrates. Even the semiconductors that are available as large single crystals present challenges to conventional compression tests; since semiconductor alloys are so brittle, all meaningful compression tests must be performed at elevated temperatures. For semiconductor alloys that are only available as thin films, hardness measurements are the only practical measurements of mechanical properties. Also, as indicated by Dr. Marcie Berding of SRI International [11], the structurally related properties of interest in semiconductors are the reduction of dislocations, elastic constants, resistance to thermal stress, adhesion to substrates, and the effects of phase transformations on properties. A quantitative understanding of the plastic behavior of semiconductor alloys will lead to an understanding of the structural properties. In summary, hardness measurements are the only easily measured mechanical property for most semiconductor alloys and they provide a good basis for understanding the complex plastic behavior in semiconductors.

## III. Growth of GaPAs epitaxial layers

The isothermal vapor phase epitaxial (ISOVPE) method was pioneered by Marfaing

et al. [12] and Fleming [13] recently refined the method. This method has been used to grow good quality, thick films (5-100  $\mu\text{m}$ ) of  $\text{Hg}_{1-x}\text{Cd}_x\text{Te}$  of varying composition (see the annual report for details). It is possible that the ISOVPE method can be used for other systems [12, 14]. The limitations are lattice mismatch and the relative vapor pressures of the components.

GaP and GaAs have a lattice mismatch of 3.7% and high vapor pressures (the vapor pressure of GaP is greater than that of GaAs [15]). We have explored the use of the ISOVPE method to grow thick films of GaPAs using a GaAs wafer as the substrate and polycrystalline GaP as the source. The experiment was performed at 675° C for 70 hours. There was only a thin film of Ga on the GaAs substrate, as indicated by scanning electron microscope EDAX analysis. Either the Ga is deposited from the GaP source or As is depleted from the GaAs substrate.

The ISOVPE experiment will be performed at a higher temperature. If this is also unsuccessful, we will try an alternate experiment consisting of a junction of GaP and GaAs substrates annealed at constant temperature. The As and P interdiffuse and should give two substrates of varying compositions near the junction surfaces. Microhardness measurements can be performed on these substrates.

#### IV. Vickers hardness of ZnTe

We reported hardness values versus composition for  $\text{Zn}_x\text{Cd}_{1-x}\text{Te}$  alloys in our first annual report. We used a hardness value of 82  $\text{kg/mm}^2$  for ZnTe from Goryunova et al. [16]. A large grained bulk sample of ZnTe was grown here at Stanford by the Bridgman method. The sample was mounted in epoxy, mechanically polished, and analyzed by EDAX on the SEM to verify its composition. Vickers hardness measurements were made in several grains, giving an average hardness value of 66  $\text{kg/mm}^2$  with a standard deviation of 2.3  $\text{kg/mm}^2$ . If we compare our value to that of Goryunova et al. [16], we see that our value is 22% lower than theirs. This difference is typical of the scatter in hardness in the

literature. For example, we encountered this problem while searching the literature for hardness values of CdTe; the values range from 43 kg/mm<sup>2</sup> to 72 kg/mm<sup>2</sup>. Our hardness value of 66 kg/mm<sup>2</sup> for ZnTe makes the strengthening effect seen in the ternary Zn<sub>x</sub>Cd<sub>1-x</sub>Te alloys even more pronounced.

#### V. Nanoindenter studies

Most films prepared by MBE or MOCVD are less than 0.1 μm thick and conventional microhardness measurements cannot be made on such thin films. Meaningful hardness measurements can be made on such films using a new instrument, the nanoindenter. The nanoindenter has several advantages: hardness can be obtained over a small area and on very thin films; indentation imaging is not needed; the indentation rate can be varied; and hardness can be monitored continuously with depth. Important capabilities of the nanoindenter include a minimum indentation depth of 200 Å; force resolution of 0.5 mN; displacement resolution of 2 Å; and a typical indentation rate of 30 Å/sec [17].

Two sets of samples were tested using the nanoindenter: Hg<sub>1-x</sub>Cd<sub>x</sub>Te and Hg<sub>1-x</sub>Zn<sub>x</sub>Te epilayers grown on Zn<sub>x</sub>Cd<sub>1-x</sub>Te substrates by LPE; and ZnTe-CdTe superlattices grown by MOCVD. Dr. Mitra Sen of the Santa Barbara Research Center provided the HgCdTe and HgZnTe samples, and Dr. David Kisker of Bell Labs supplied the superlattice samples.

The four epilayer samples are: (1) an 11.0 μm Hg<sub>0.67</sub>Cd<sub>0.33</sub>Te epilayer on a Cd<sub>0.96</sub>Zn<sub>0.04</sub>Te substrate (MCT1); (2) a 26.0 μm Hg<sub>0.8</sub>Cd<sub>0.2</sub>Te epilayer on a Cd<sub>0.96</sub>Zn<sub>0.04</sub>Te substrate (MCT2); (3) a 7.7 μm Hg<sub>0.76</sub>Zn<sub>0.24</sub>Te epilayer on a Cd<sub>0.76</sub>Zn<sub>0.24</sub>Te substrate (MZT1); and (4) an 11.0 μm Hg<sub>0.84</sub>Zn<sub>0.16</sub>Te epilayer on a Cd<sub>0.74</sub>Zn<sub>0.26</sub>Te substrate (MZT2). Table 1 gives values of hardness versus plastic depth for the four samples. The two HgCdTe epilayer samples range in hardness from 116 kg/mm<sup>2</sup> to 67 kg/mm<sup>2</sup> for x=0.33 (MCT1) and from 111 kg/mm<sup>2</sup> to 64 kg/mm<sup>2</sup> for x=0.2 (MCT2). The hardness depends on plastic depth--smaller depths (i.e., smaller loads)



usually give higher hardness values. Vickers hardness measurements were performed on the  $\text{Hg}_{0.8}\text{Cd}_{0.2}\text{Te}$  epilayer sample (MCT2) since it is sufficiently thick. The average Vickers hardness is  $54.5 \text{ kg/mm}^2$  with a standard deviation of  $3.4 \text{ kg/mm}^2$ , compared to the nanoindenter hardness measurements for that sample which range from 111 to  $64 \text{ kg/mm}^2$ . Two sets of hardness measurements were performed in different regions on the  $\text{Hg}_{0.76}\text{Zn}_{0.24}\text{Te}$  epilayer sample (MZT1). The hardness values range from  $140 \text{ kg/mm}^2$  to  $122 \text{ kg/mm}^2$  in one region and from  $178 \text{ kg/mm}^2$  to  $155 \text{ kg/mm}^2$  in the other region. These differences in hardness values between two regions on the same sample can be explained by the poor surface quality of the epilayer and possible compositional variations over the epilayer. The surface quality of the  $\text{Hg}_{0.84}\text{Zn}_{0.16}\text{Te}$  epilayer sample (MZT2) was so poor that hardness measurements could be made at only two depths. The hardness values range from  $162 \text{ kg/mm}^2$  to  $134 \text{ kg/mm}^2$  at plastic depths of 89.5 nm and 875.8 nm, respectively. Although there is a small difference between the individual  $\text{HgCdTe}$  samples and individual  $\text{HgZnTe}$  samples, these results clearly show that the  $\text{HgZnTe}$  samples are harder (about 35%) than the  $\text{HgCdTe}$  samples. (See figure 1.)

One may calculate "compliance" values from the linear unloading portion of the load versus depth curves of the nanoindenter tests. Table 2 gives these "compliance" values for each plastic depth. If the "compliance" is plotted as a function of the inverse of the plastic depth, the result is a straight line whose slope can be used to calculate the Young's modulus for that sample. Figure 2 shows the "compliance" values versus the  $1/\text{plastic depth}$  values. The y intercept values, which are a measure of the compliance of the loading column and any additional compliance associated with the mounting of the sample, cluster around  $3\text{-}7 \text{ nm/mN}$ , except for the MCT1 sample, whose y intercept is  $20 \text{ nm/mN}$ . We believe that this sample might not have been mounted as securely as the other samples, but this should not affect the validity of the hardness values or the modulus values. Hardness is measured as the indenter encounters resistance, so hardness is not influenced by the sample mounting. The modulus values are calculated from the slope of the "compliance" as

a function of the inverse of the plastic depth, so the intercept value is not important. Table 2 also gives the calculated values for the Young's modulus for the samples. They measure 62.2-62.6 GPa for the two HgCdTe samples and from 66.8 GPa to 67.6 GPa for the two HgZnTe samples. Simmons and Wang [18] give Young's modulus values of 35-42 GPa for CdTe, 35-42 GPa for HgTe, and 61 GPa for ZnTe. The modulus values for the HgCdTe samples are almost twice the literature values for HgTe and CdTe. The modulus values for the HgZnTe samples are very close to the literature value for pure ZnTe.

Two ZnTe-CdTe superlattice samples were also measured on the nanoindenter. The samples are: (1) sample 870827-1, a GaAs substrate with a 1.0  $\mu\text{m}$  ZnTe buffer layer, 200 cycles of 25  $\text{\AA}$  CdTe and 50  $\text{\AA}$  ZnTe, and a 50  $\text{\AA}$  CdTe cap; and (2) sample 870629-2, a GaAs substrate with a 1.0  $\mu\text{m}$  ZnTe buffer layer, 40 cycles of 25  $\text{\AA}$  CdTe and 50  $\text{\AA}$  ZnTe, and a 50  $\text{\AA}$  CdTe cap. Table 3 shows the hardness values at the corresponding plastic depths and the calculated values for the Young's modulus. Each hardness value in the table is the average of five measurements (except for test 27A, which was terminated prematurely due to a software error) and the standard deviation is in parenthesis. Figure 3 shows the hardness versus plastic depth (i.e., load) for sample 870827-1. The error bars represent  $\pm$  one standard deviation. Figure 4 is a graph of hardness versus plastic depth for sample 870629-2. Figure 5 is a graph of hardness versus plastic depth for both samples without the error bars. Figure 6 shows "compliance" values versus the inverse of the plastic depth for the five tests on the two samples.

There are several major results from these tests. The hardness values for both superlattice samples are much higher than the Vickers hardness values for CdTe and ZnTe samples. The hardness values for sample 870827-1 range from 283  $\text{kg/mm}^2$  to 213  $\text{kg/mm}^2$  (depending on depth), while those for sample 870629-2 range from 254  $\text{kg/mm}^2$  to 162  $\text{kg/mm}^2$  (depending on depth). Vickers hardness values of CdTe and ZnTe samples are 46  $\text{kg/mm}^2$  and 65  $\text{kg/mm}^2$ , respectively. The hardness values of the "thicker" superlattice sample (870827-1, the sample with more layers) are higher than those of the

"thinner" superlattice sample (870629-2). Also, the hardness values of the "thicker" superlattice sample decrease with increasing depth (i.e., load), as is usually observed for most metal and semiconductor samples, but then increase again, which is not expected. Cracking is seen at the higher loads and may be affecting the hardness.

The Young's modulus values for the two superlattice samples are similar (99.6 GPa with a standard deviation of 22.2 GPa for sample 870827-1 and 119.4 GPa with a standard deviation of 4.4 GPa for sample 870629-2), but both values are higher than the literature values for CdTe and ZnTe (35-42 GPa for CdTe and 61 GPa for ZnTe [18]). If the modulus values for the superlattices are higher than those for the corresponding annealed samples, this may be an example of the "supermodulus effect." This effect (a significant increase in Young's modulus due to multilayers) has been seen in several metallic superlattices (e.g., Au/Ni, Cu/Pd, Cu/Ni, and Ag/Pd [19-21]). The possible supermodulus effect will be studied further by hardness tests on the corresponding annealed superlattice samples.

## VI. Bulk growth of $\text{Ga}_x\text{In}_{1-x}\text{Sb}$

The pseudobinary semiconductor,  $\text{Ga}_x\text{In}_{1-x}\text{Sb}$ , was chosen for bulk growth because the melting temperature is fairly low and because there is information in the literature on the growth of this system arising from an interest in its use for Gunn devices and three-level oscillators [22]. Single crystal growth of  $\text{Ga}_x\text{In}_{1-x}\text{Sb}$  is difficult because of the high segregation of GaSb in InSb, interface breakdown due to constitutional supercooling, and low diffusion rates in the material [23]; however, we have obtained coarse grained samples of varying composition suitable for microhardness measurements.

A bulk sample was grown by a vertical Bridgman technique using an encapsulated crucible. The liquid was homogenized by a five day anneal and growth was made at a 0.8 mm/day rate. The ingot was then removed and sectioned. The ingot is polycrystalline with long columnar grains (some as long as 15-20 mm) about 2-4 mm in diameter. Microprobe

analysis was performed on the ingot, giving the composition profile seen in figure 7. Vickers hardness measurements were also performed on the ingot.

Figure 8 shows hardness versus composition in  $\text{Ga}_x\text{In}_{1-x}\text{Sb}$ . The data include values from the first GaInSb ingot. Figure 8 also shows literature values [16] for the two binary semiconductors and three ternary alloy samples. The results are interesting--our hardness values show no strengthening in the ternary alloys, other than that predicted by a linear hardening law. The bowing of the hardness curve seen by Goryunova et al. [16] is not seen in our data. Future possible work on this system includes hardness measurements on GaSb and InSb to complete our hardness versus composition curve.

## VII. Future work

Proposed work in the near future includes: collaboration with Professor Fred Pollak of CUNY to determine the Raman spectra of ISOVPE-grown epilayers of HgCdTe of varying composition; hardness measurements using the nanoindenter on annealed ZnTe-CdTe superlattice samples; hardness measurements using the nanoindenter on Si-Ge strained layer superlattices and the corresponding annealed samples; and junction experiments to supplement the ternary systems where the ISOVPE method is not successful. We are also investigating the possibility of building a hardness testing device which would modify a Vickers hardness machine to allow the measuring and recording of load versus depth during hardness tests.

## References

1. A. Sher, A. Chen, W. E. Spicer, and C. Shik, Proceedings of the 1984 U.S. Workshop on the Physics and Chemistry of Mercury Cadmium Telluride: American Vacuum Society and American Institute of Physics (1985), T. Casselman, editor.
2. M. C. Flemings, Solidification Processing, McGraw Hill (1973), p. 64.
3. W. W. Mullins and R. F. Sekerka, J. Appl. Phys., 34:323 (1963); 35:444 (1964).
4. R. F. Sekerka, J. Appl. Phys., 36:264 (1965).
5. R. F. Sekerka, J. Phys. Chem. Solids, 28:983 (1967).
6. R. F. Sekerka, J. Crystal Growth, 3:71 (1968).
7. Ing. H. Bückle, Metallurgical Reviews, 4:49 (1959).
8. G. E. Dieter, Mechanical Metallurgy, McGraw Hill, Inc. 1976.
9. D. Tabor, Proceedings of the Institute of Physics, F. Physics in Technology, 1:145 (1970).
10. D. Tabor, Microindentation Techniques in Materials Science and Engineering, ASTM STP 889, P. J. Blau and B. R. Lawn, editors, American Society for Testing and Materials, Philadelphia, 1986, pp. 129-159.
11. M. Berding, SRI International, in letter to Captain K. Malloy, AFOSR, October 14, 1987.
12. Y. Marfaing, G. Cohen-Solal, and F. Bailly, Proceedings of an International Conference on Crystal Growth, Boston, 20-24 June 1966, H. S. Peiser, editor.

13. J. G. Fleming, Growth and Properties of Mercury Cadmium Telluride Investigated Using Isothermal Techniques, Ph.D. dissertation, Stanford University, September 1986.
14. M. H. Kalisher, Santa Barbara Research Center, personal communication.
15. C. D. Thurmond, J. Phys. Chem. Solids, 26:785 (1965).
16. N. A. Goryunova, A. S. Borshchevskii, and D. N. Tretiakov, Semiconductors and Semimetals, vol. 4, Physics of III-V Compounds, 1968, R. K. Willardson and A. C. Beer, editors, pp. 3-34.
17. M. F. Doerner and W. D. Nix, J. Mater. Res., 1:601 (1986).
18. Simmons and Wang, Single Crystal Elastic Constants and Calculated Aggregate Properties: a Handbook, MIT Press, 2nd edition, 1971.
19. W. M. C. Yang, T. Tsakalakos, and J. E. Hilliard, J. Appl. Phys., 48:876 (1977).
20. T. Tsakalakos and J. E. Hilliard, J. Appl. Phys., 54:734 (1983).
21. G. E. Henein and J. E. Hilliard, J. Appl. Phys., 54:728 (1983).
22. A. Joullie, P. Esquirol, and G. Bougnot, Mat. Res. Bull., 9:641 (1974).
23. A. Joullie, J. Allegre, and G. Bougnot, Mat. Res. Bull., 7:1101 (1972).

Publications during April 15, 1987-April 14, 1988

1. J. G. Fleming, L. J. Farthing, and D. A. Stevenson. "Vickers Hardness of  $\text{Hg}_{1-x}\text{Cd}_x\text{Te}$  Epilayers Grown by Isothermal Vapor Phase Epitaxy," J. Crystal Growth, January 1988.
2. E. J. Smith, S. Sen, M. T. Smith, C. R. Curtis, L. J. Farthing, T. Weihs, M. F. S. Tang, and D. A. Stevenson. "Growth and Characterization of Bulk and Epitaxial  $\text{HgZnTe}$ ," IRIS paper, June 1987.
3. E. J. Smith, S. Sen, M. T. Smith, C. R. Curtis, M. F. S. Tang, T. Weihs, L. J. Farthing, and D. A. Stevenson. "Growth and Characterization of Bulk and Epitaxial  $\text{HgZnTe}$ ," presented at the Seventh American Conference on Crystal Growth, July 12-17, 1987, Monterey, California.

Table 1. Hardness as a function of plastic depth for epilayer samples

Sample	H <sub>plastic</sub> (nm)	Hardness (GPa)	Hardness (kg/mm <sup>2</sup> )
Hg <sub>0.67</sub> Cd <sub>0.33</sub> Te	86.6	1.159	116
epilayer on	170.9	1.003	100
Cd <sub>0.96</sub> Zn <sub>0.04</sub> Te	405.2	0.796	80
substrate (HCT1)	763.9	0.672	67
Hg <sub>0.8</sub> Cd <sub>0.2</sub> Te	92.9	1.108	111
epilayer on	185.3	0.966	97
Cd <sub>0.96</sub> Zn <sub>0.04</sub> Te	461.9	0.787	79
substrate (HCT2)	905.1	0.694	64
Hg <sub>0.76</sub> Zn <sub>0.24</sub> Te	92.8	1.396	140
epilayer on	185.8	1.251	125
Cd <sub>0.76</sub> Zn <sub>0.24</sub> Te	452.7	1.310	131
substrate (HCT1)	885.6	1.221	122
	87.9	1.779	178
	87.7	1.783	178
	178.8	1.615	162
	440.1	1.567	157
	839.1	1.555	156
	853.9	1.552	155
Hg <sub>0.84</sub> Zn <sub>0.16</sub> Te	89.5	1.619	162
epilayer on	875.8	1.338	134
Cd <sub>0.74</sub> Zn <sub>0.26</sub> Te			
substrate (HCT2)			



Table 2. "Compliance" as a function of plastic depth and Young's modulus values for epilayer samples

Sample	H <sub>plastic</sub> (nm)	"Compliance" (nm/mN)	Young's modulus (GPa)
Hg <sub>0.67</sub> Cd <sub>0.33</sub> Te epilayer on Cd <sub>0.96</sub> Zn <sub>0.04</sub> Te substrate (HCT1)	86.6	53.63	62.2
	170.9	39.16	
	405.2	28.94	
	763.9	25.00	
Hg <sub>0.8</sub> Cd <sub>0.2</sub> Te epilayer on Cd <sub>0.96</sub> Zn <sub>0.04</sub> Te substrate (HCT2)	92.9	34.37	62.6
	185.3	20.75	
	461.9	10.86	
	905.1	7.69	
Hg <sub>0.76</sub> Zn <sub>0.24</sub> Te epilayer on Cd <sub>0.76</sub> Zn <sub>0.24</sub> Te substrate (HZT1)	92.8	28.39	69.4
	185.8	15.90	
	452.7	7.13	
	885.6	4.11	
	87.9	32.19	65.8
	87.7	31.06	
	178.8	17.12	
	440.1	7.65	
	839.1	5.13	
	853.9	4.31	
Hg <sub>0.84</sub> Zn <sub>0.16</sub> Te epilayer on Cd <sub>0.74</sub> Zn <sub>0.26</sub> Te substrate (HZT2)	89.5	30.28	66.8
	875.8	4.20	

Table 3. Hardness and Young's modulus values for two ZnTe-CdTe superlattice samples

Sample	Plastic depth (nm)	Hardness* (GPa)	Hardness (kg/mm <sup>2</sup> )	Young's modulus (GPa)
870827-1 27A	84.4	2.662	266	83.8
	173.0	2.536	254	
	356.6	2.063	206	
	594.5	2.148	215	
	1215.8	2.413	241	
27B1	32.0	2.833 (0.530)	283	125.0
	49.2	2.660 (0.186)	266	
	65.5	2.708 (0.311)	271	
	82.3	2.816 (0.166)	282	
	258.6	2.262 (0.121)	226	
27B2	83.7	2.786 (0.213)	279	90.0
	170.5	2.544 (0.140)	254	
	351.7	2.127 (0.083)	213	
	686.2	2.254 (0.110)	225	
	1187.9	2.667 (0.141)	267	
870629-2 29C	33.4	2.535 (0.328)	254	116.2
	51.6	2.354 (0.216)	235	
	71.1	2.154 (0.083)	215	
	90.3	1.903 (0.156)	190	
	275.3	1.722 (0.099)	172	

29D	34.3	2.400 (0.235)	240	122.5
	52.8	2.153 (0.144)	215	
	72.1	1.944 (0.115)	194	
	91.4	1.943 (0.139)	194	
	277.0	1.624 (0.136)	162	

\* Each hardness value is the average of five measurements and the standard deviation is in parenthesis.

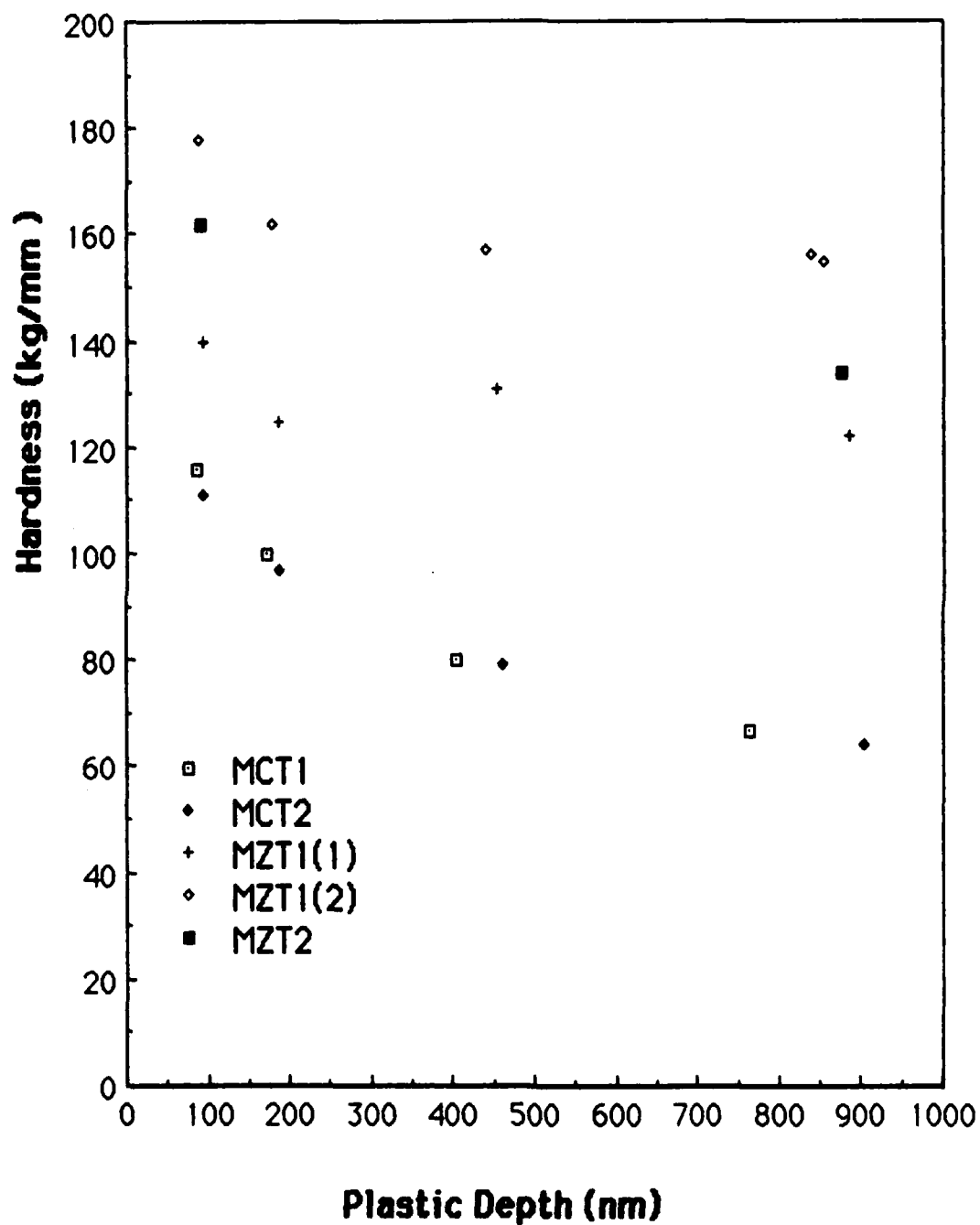


Figure 1. Hardness versus plastic depth for two MCT and two MZT samples

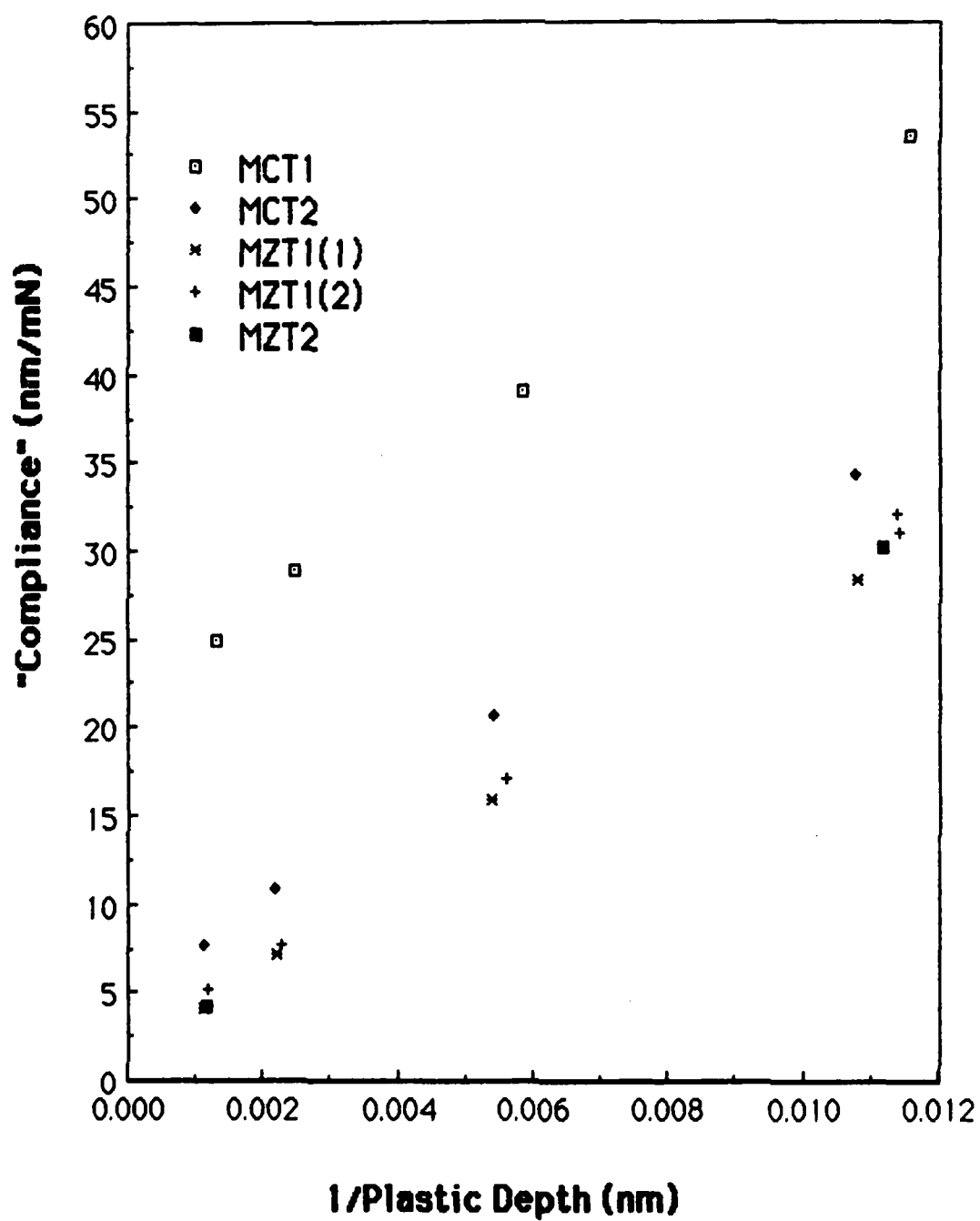


Figure 2. "Compliance" versus inverse plastic depth for two MCT and two MZT samples

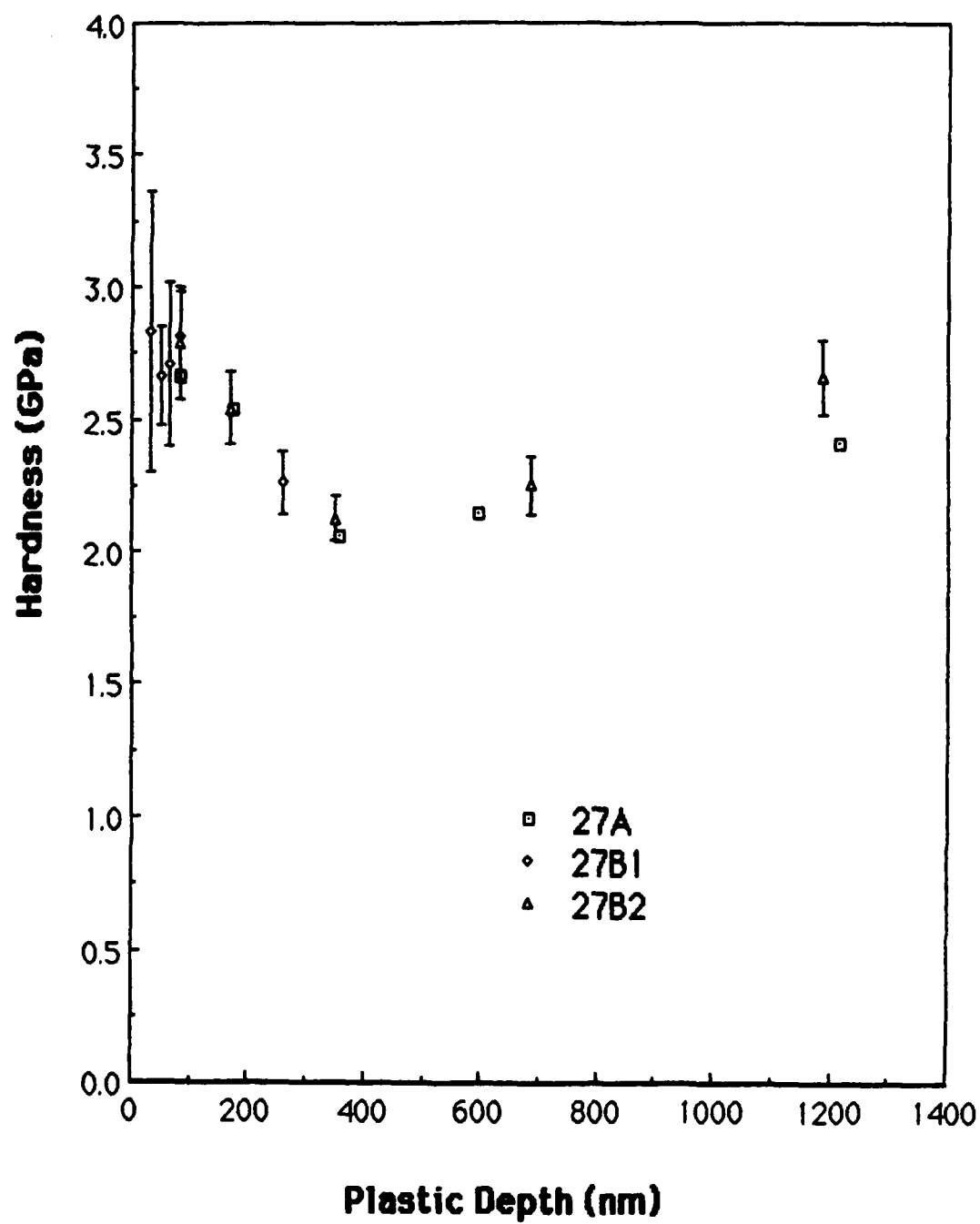


Figure 3. Hardness versus plastic depth for ZnTe-CdTe superlattice sample 870827-1

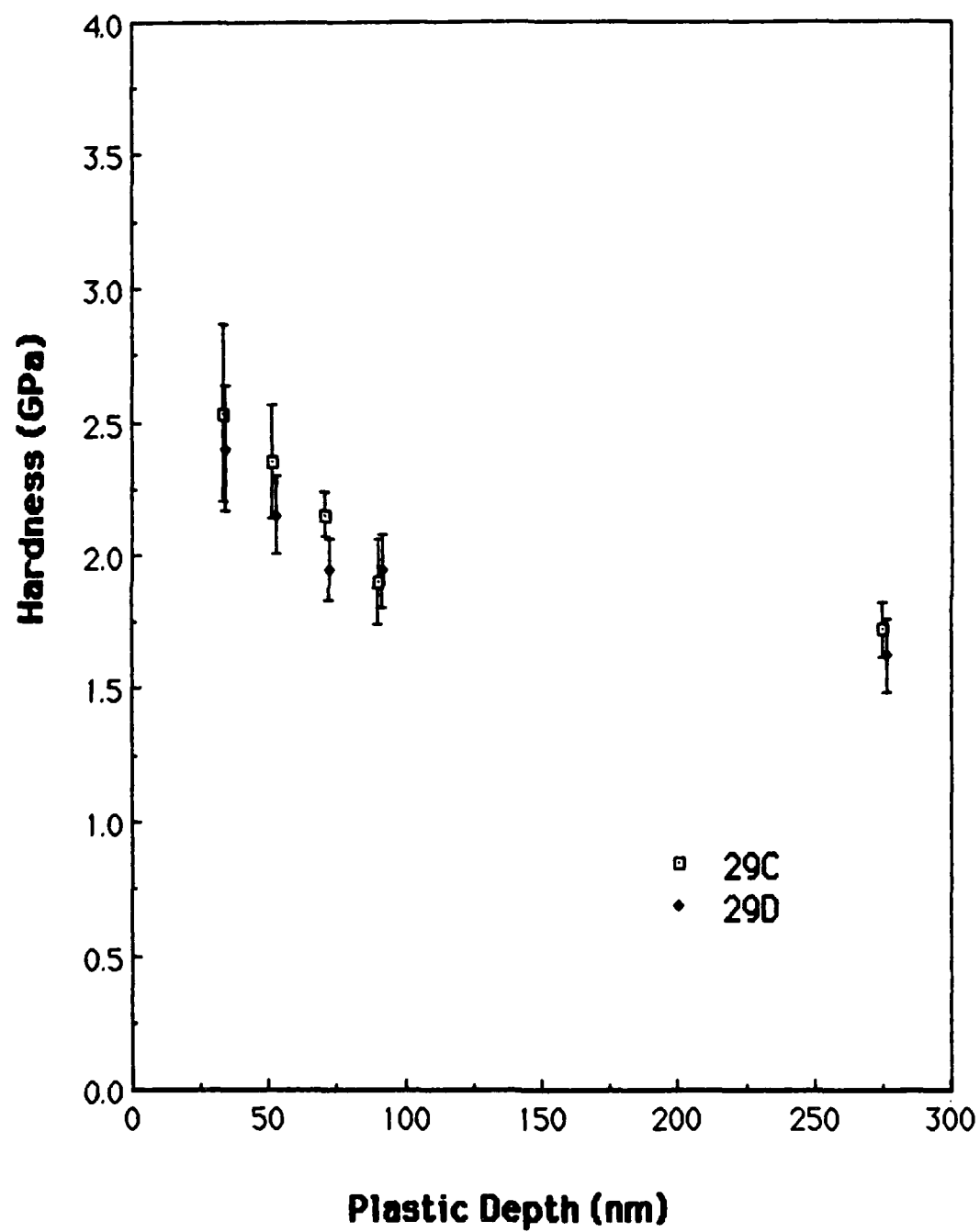


Figure 4. Hardness versus plastic depth for ZnTe-CdTe superlattice sample 870629-2

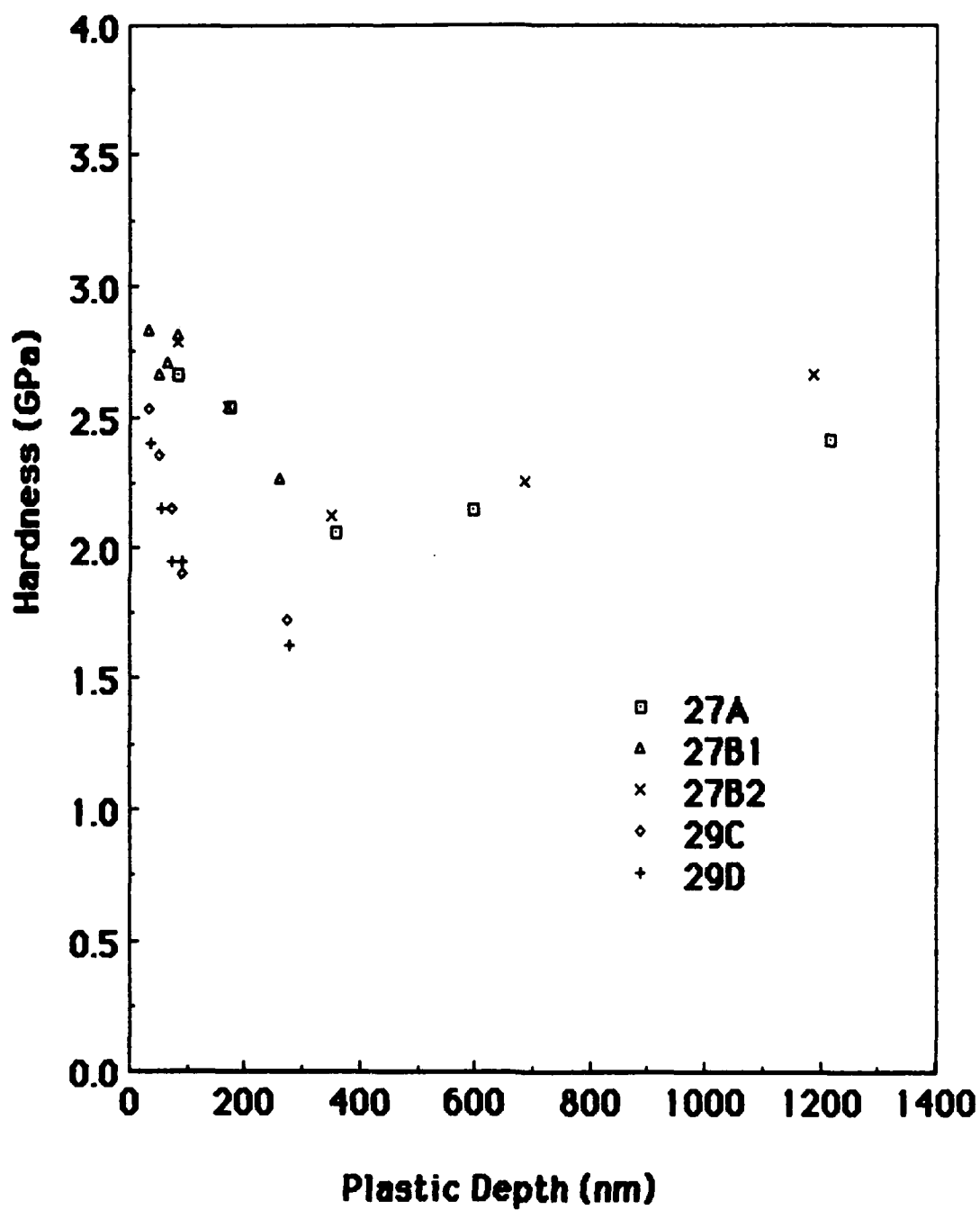


Figure 5. Hardness versus plastic depth for ZnTe-CdTe superlattice samples 870827-1 and 870629-2



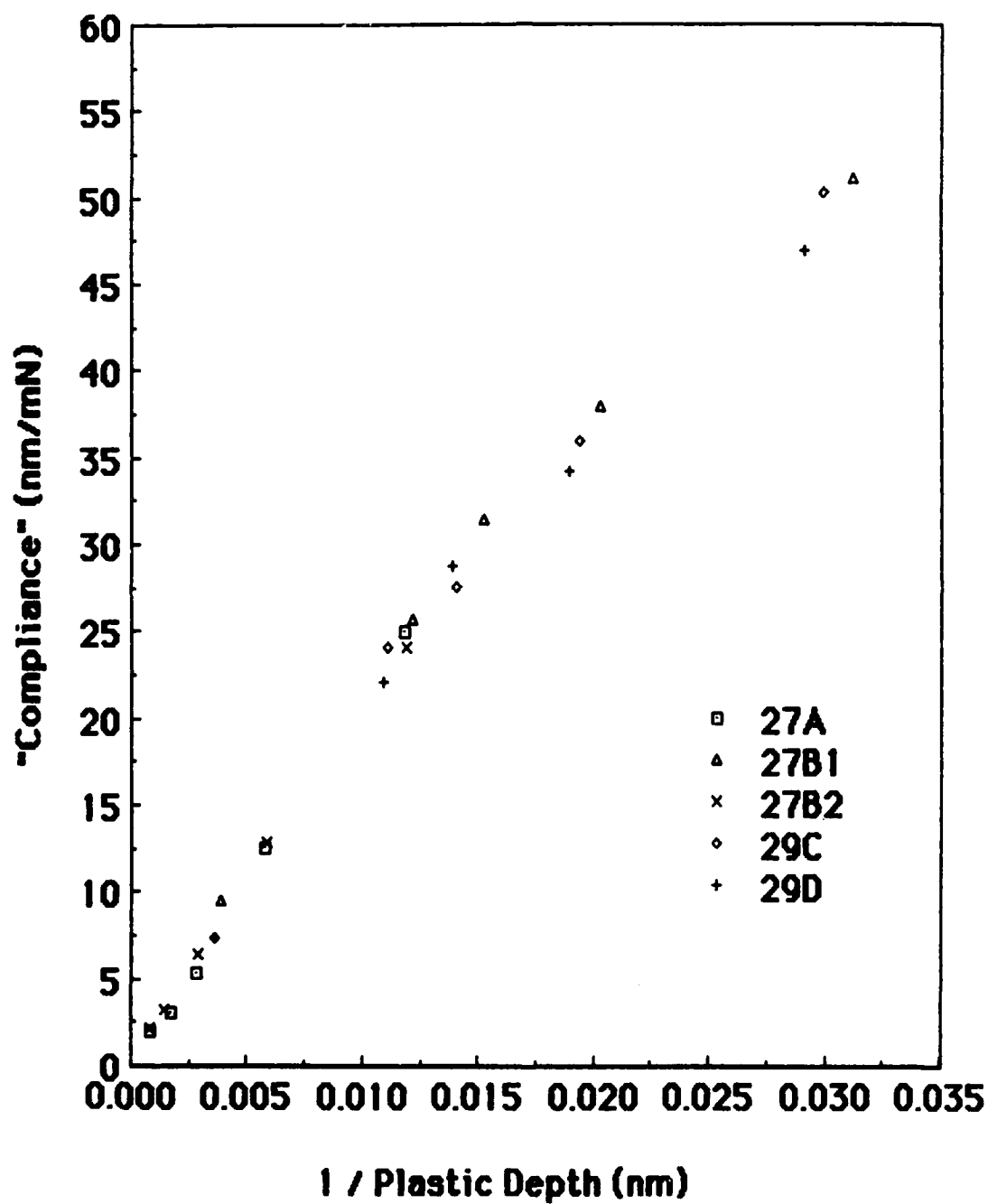


Figure 6. "Compliance" versus inverse plastic depth for ZnTe-CdTe superlattice samples 870827-1 and 870629-2

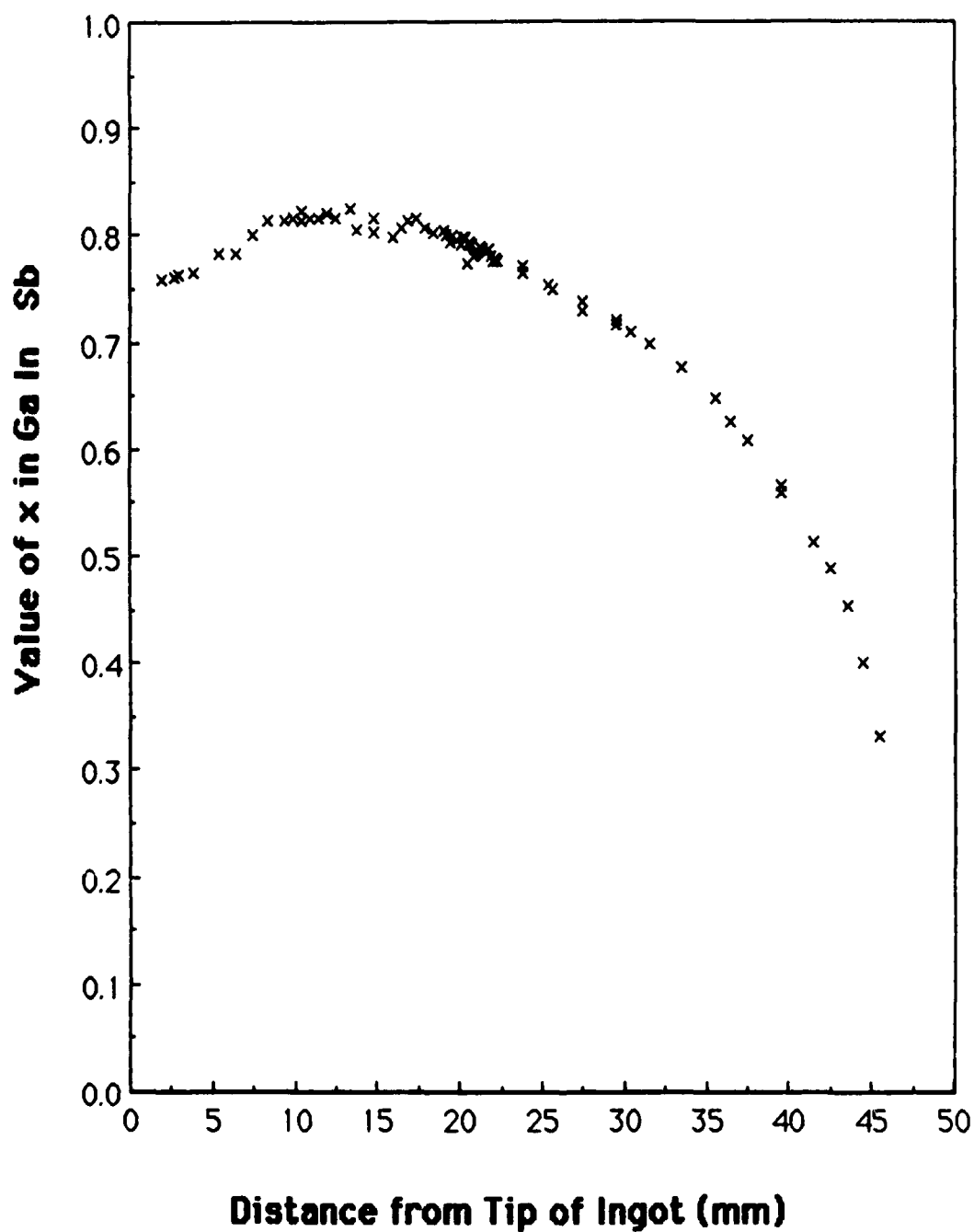


Figure 7.  $x$  value in  $\text{Ga}_x\text{In}_{1-x}\text{Sb}$  ingot #2 versus distance from tip of ingot

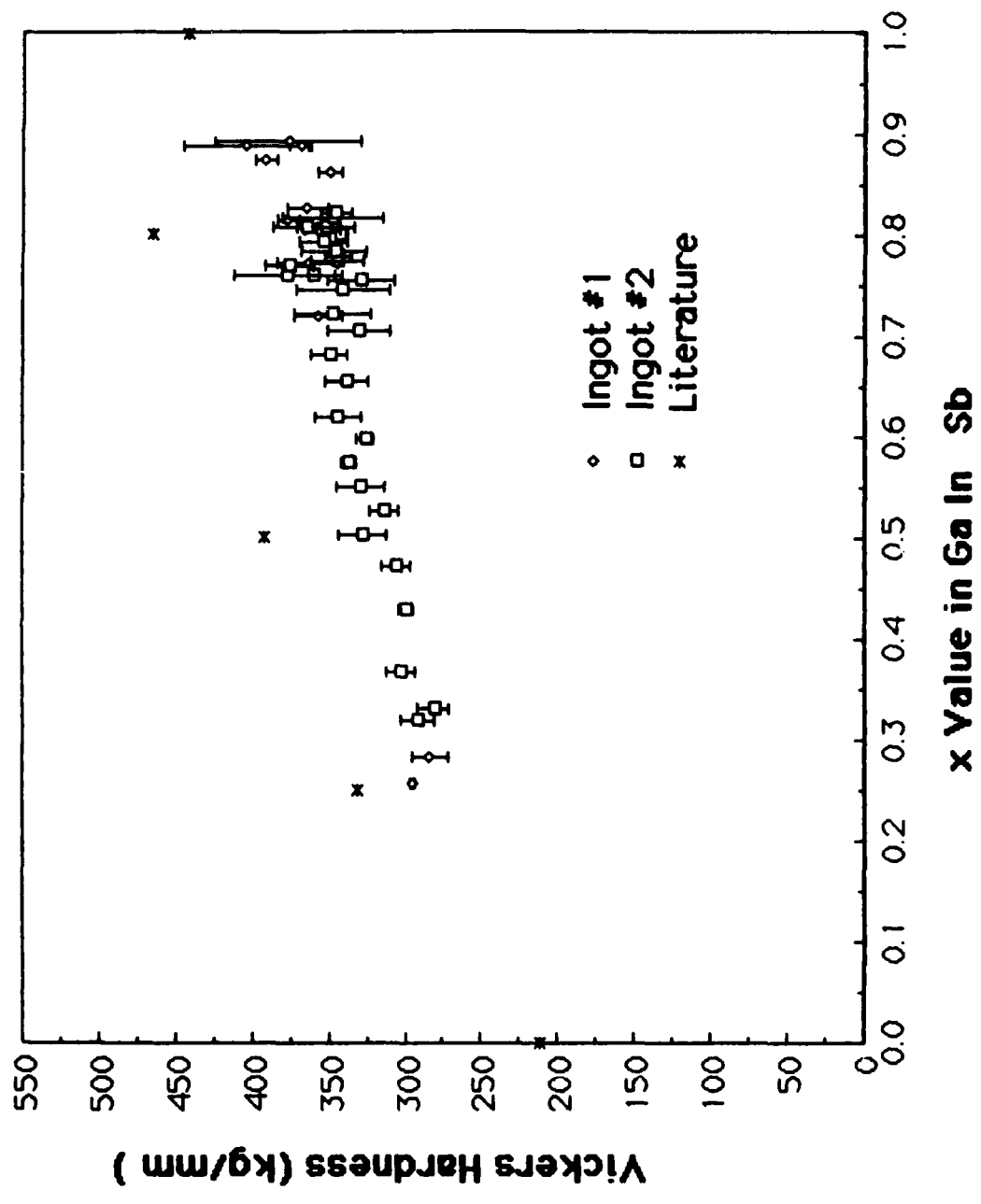


Figure 8. Vickers hardness as a function of x in  $\text{Ga}_x\text{In}_{1-x}\text{Sb}$

END

DATE

FILMED

DTIC

10-88